Advanced Processing and Manufacturing

DEVELOPMENT OF HIGH TEMPERATURE JOINING AND THERMOMECHANICAL CHARACTERIZATION APPROACHES FOR SiC/SiC COMPOSITES

Michael C. Halbig[1], Mrityunjay Singh[2], and Jerry Lang[1]
[1] NASA Glenn Research Center, Cleveland, OH
[2] Ohio Aerospace Institute, Cleveland, OH

ABSTRACT

Advanced joining technologies are enabling for the fabrication of large and complex shaped silicon carbide-based ceramic and ceramic matrix composite components to be utilized in high temperature extreme environment applications. Many joining approaches are being proposed and developed. New standardized tests are needed to fully characterize joint properties and capabilities. One such test ISO-13124, was used for mechanical testing in this work. This test configuration allows for testing of joined crossbars in either a tensile or a shear stress state. The REABond joining approach using Si-8.5%Hf eutectic phase alloy was used to join ceramic matrix composite and monolithic silicon carbide materials. In mechanical testing, low strengths were obtained with failures occurring in the joined substrates. Finite element analysis of the stress states revealed stresses concentrations at the edges of up to 30 times higher than the 2 MPa nominal stress for the tensile state. For the shear state, out of plane displacements occurred.

INTRODUCTION

Silicon carbide fiber reinforced / silicon carbide matrix composites (SiC/SiC) are a class of ceramic matrix composite (CMC) materials are being developed for turbine engine applications for such components as combustor liners, shrouds, vanes, and blades[1-4]. These CMC components can operate at higher temperatures, require less cooling, and are lighter weight than metal components. The use of CMCs in such applications contributes to increased turbine engine fuel efficiencies, reduced emissions, and long term durability. As interest in fiber reinforced SiC-based composite materials continues to grow due to advancements in their properties, new integration technologies and testing capabilities will be critically needed.

In order to evaluate the mechanical properties of joints, standardized tests and testing capabilities are needed. One such standardized test[5], BS-ISO-13124:2011, "Fine ceramics (advanced ceramics, advanced technical ceramics): Test method for interfacial bond strength of ceramic materials," was applied for evaluation of mechanical properties of monolithic SiC and SiC/SiC materials joined to themselves. In this test, two long rectangular substrates are bonded across one another at their midsection to form an "X" shaped crossbar to provide samples for testing either in a tensile stress state or a shear stress state. Due to the need for multiple crossbars for testing and because of the unique shape, a simple joining approach was needed for processing the joints. The authors had previously reported a diffusion bonding approach for joining SiC based materials using titanium interlayers[6-7]. However, such an approach needs relatively smooth surfaces and requires high applied loads from a hot press to aid in bond formation. Another joining approach, Refractory Eutectic Assisted BONDing (REABOND) was used for evaluating joints according to ISO-13124. REABond uses Si-8.5Hf eutectic phase allow powder in a green tape for the joining interlayer. During joint processing, no load is needed and the eutectic phase melts to flow over the substrate surface and solidifies during cooling. REBOND has been demonstrated on the joining of SiC/SiC composites resulting dense, crack free joints that filled the contour of the rough CMC surface[8].

Joining of SiC/SiC substrates and monolithic SiC was conducted to support the mechanical test method development. Microstructural analysis was conducted using optical microscopy and scanning electron microscopy (SEM) coupled with energy dispersive spectroscopy (EDS) to

evaluate bond quality. Mechanical tests were conducted at room temperature according to ISO-13124 for testing joints under tensile or shear stress conditions.

In correlation to the experimental tests, the test standard was evaluated in a finite element model investigation. The purpose of the investigation was to determine the reliability of the interfacial bond strength test for two types of test methods for the ISO-13124, by characterizing the stress state within the bond region by finite element methods. The objective was to determine the stress concentration within the bond region so that a more accurate stress measurement can be determined from the experimental test results of the tensile and shear specimens. Knowing this stress state would better characterize the strength of the ceramic bond and would help determine if any modifications were needed to the specimen and/or test setup while still remaining compliant to the ISO-13124 standard for fine and advance ceramics interfacial bond strength test method.

EXPERIMENTAL

The CMCs were two different types of silicon carbide fiber/silicon carbide matrix (SiC/SiC) CMCs. The first CMC was SiC/SiC HiPerComp™ Gen II by GE Energy (Newark, DE). The SiC fibers were Hi-Nicalon Type-S. The SiC matrix was manufactured by the prepreg melt infiltration method[9]. The second CMC was melt infiltrated (MI) SiC/SiC fabricated by Goodrich Corporation (CA) using Hi-Nicalon SiC fibers with a BN/SiC interface. Both SiC/SiC materials had a 0º/90º woven fiber tow architecture. Due to lower than expected mechanical strength results from the joined CMC materials, joining of monolithic SiC substrates was also conducted. The purpose was to eliminate the added complication of low interlaminar properties which are typical of CMCs.

REABond green tapes were prepared for use as the interlayer for joining. Previously several eutectic phase alloys were evaluated and the Si-8.5Hf eutectic phase alloy was down-selected as giving the best results for joining CMCs[8]. For the current effort, powders of less than 70 microns in diameter of the Si-8.5Hf eutectic phase alloy were mixed with binders to prepare the green tapes by tape casting. The tapes had a solid loading of about 30-35% and were 0.21 mm thick. A second set of tapes were prepared with 5 wt.% of SiC nanofibers integrated in with the eutectic powders. The SiC nanofibers were approximately 0.15 microns in diameter and 10 microns in length. The SiC nanofibers were produced at NASA GRC[10].

The substrates were rectangular bar shapes that had been machined from larger coupons. Joining of two bars at the crossover of their midsection as illustrated in Figure 1, forms the cross-bar shape for testing according to the ISO-13124 standard. The test standard recommends test bars that have dimensions of 12 mm x 4 mm x 4 mm. The test standard and the recommended sample size was developed for standardized testing of monolithic ceramics. However, since the standard is being applied here to the testing of CMCs, the small 4 mm x 4 mm crossover area was increased so that repeating unit cells of the fiber architecture could be present within the bond area to maximize the benefit of the fiber architecture. Therefor the bar size was doubled to 24 mm x 8 mm x 8 mm. However, actual dimensions of the CMC test bars varied due to the sizes of available CMC coupons. The dimensions in the length x width x height were roughly 24 mm x 6 mm x 2 mm for the GE SiC/SiC, 24 mm x 8 mm x 2.5 mm for the BFG SiC/SiC, and 33 mm x 6.4 mm x 3.2 mm for the monolithic SiC material.

Green tapes of each type, with nanotubes and without, were cut to match the mating surface area of the substrates being joined. Multiple layers of the green tape were used to achieve an interlayer thickness suitable for filling in the surface voids of the paired substrates which arise due to surface roughness from the fiber architecture. Therefore, two green tapes were used to join the GE SiC/SiC and SiC monolithic materials since they were relatively smooth while three green tapes were stacked for use as the interlayer in joining the BFG SiC/SiC material which had a rougher surface. The fixture used to position the substrates for joining is shown in Figure 1. Joint

processing was conducted in a vacuum furnace at 1375ºC with a 5 minute hold. A slow, stepped heating rate was used to burn-off the organic binders in the eutectic tape. The microstructures of polished cross-sections of the resulting joints were analyzed using an optical microscope and a field emission scanning electron microscope (FE SEM) coupled with energy dispersive spectroscopy (EDS) for elemental analysis of reaction formed phases in the joint.

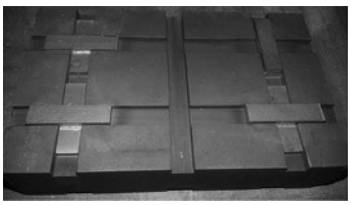

Figure 1. Image of the processing fixture that was used to join two overlapping substrates to form the crossbar configuration needed for testing according to ISO-13124. Witness samples were also joined for conducting microscopy (sample in the upper right).

The joined crossbars were tested according to the ISO-13124 standard. Figure 2 shows illustrations of the sample loading and of the crossbar configuration in the fixtures during testing for the tensile stress state (top) and the shear stress state (bottom). Fractography using a scanning electron microscope was conducted on fracture surfaces of failed samples. In some cases, failure did not occur at the joint and the joint region remained intact. In these cases, macrographs were taken to capture the failure location.

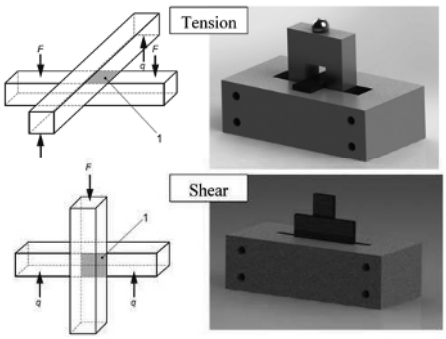

Figure 2. Illustration of the sample loading (left) and the position of the samples in the test fixtures (right) for the tensile stress state (top) and for the shear stress state (bottom).

Model Description

Two solid models were created to represent the cross-bonded specimen used in the tension strength test and the shear strength test. Two dimensional configurations existed; the BFG configuration and GE configuration. The cross-bonded specimen configuration fabricated by BFG was constructed of two ceramic matrix composite beams bonded at a 90° angle with each beam of rectangular shape with a length, width, and height of 24 mm x 8 mm x 2.51 mm, respectively. The cross-bonded specimen configuration fabricated by GE were bonded at a 90° angle with each beam

of rectangular shape with a length, width, and height of 24 mm x 6 mm x 1.96 mm, respectively. The bond area that represented the ceramic bond region in the model is 64 mm^2. The BFG cross-bonded solid model was meshed with 20-node hexahedra elements and consisted of 48,000 elements and 207,921 nodes. The GE cross-bonded specimen solid model was slightly different with a reduced bond area of 36 mm^2. The solid model was meshed using the same brick element type and consist of 48,000 elements and 207,921 nodes. Since the ceramic bond and ceramic matrix composite material properties were similar, all of the model's bonded regions were represented by modeling the adjacent beams such that the overlap region of the volumes at the surface shared the same area. The finite element models were created using the ANSYS finite element analysis code.

Analysis Description

Four finite element analyses were conducted to simulate how stresses distributed itself within the bond region. The cross-bonded specimens were configured such that both a tensile strength test and a shear strength test could be conducted by changing the orientation of the test specimen. For the finite element models that represented the BFG and GE configuration, two load cases were created for the analysis. Load case 1 represented boundary conditions and loading for the tensile bond strength test and load case 2 represented boundary conditions and loading for the shear bond strength test. Each load case applied a 1MPa load in the appropriate location and direction along with the necessary boundary constraints to replicate the type of test to be simulated. Figure 2 shows a schematic of the boundary conditions and loading setup for the two load case runs in the static analysis. The left top figure represents conditions for load case 1 and the left bottom figure represents conditions for load case 2.

RESULTS AND DISCUSSION

Analysis of the green tape prepared with 5 wt.% SiC nanotubes was conducted using a scanning electron microscope. The green tape was frozen in liquid nitrogen and then fractured to allow for analysis through the thickness of the tape. The nanotubes were well distributed within the green tape as shown in Figure 3. The nanotubes did not have a preferred orientation and were observed at various angles parallel and perpendicular to the plane of the tape. Also seen in the figure, are the relatively larger Si-8.5Hf eutectic phase powders which had previously been sieved for powders that were sized less than 70 micron in diameter. The good distribution of nanotubes was expected to provide composite like toughening to the joint region which would otherwise have properties of a monolithic ceramic.

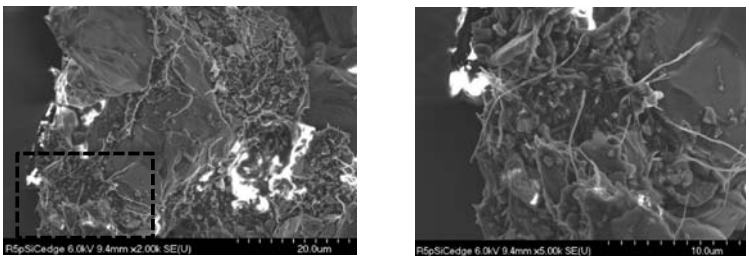

Figure 3. FE SEM micrographs of a view through the thickness of the green REABOND tape with 5 wt.% SiC nanotube additions. The same region is shown at different magnifications.

The REABond tapes provided good quality joints that were uniform, dense, and crack free. The interfaces between the substrates and joint material showed good adhesion and no gaps or

delaminations. This was the case for all three joined substrates: GE SiC/SiC, BFG SiC/SiC, and the monolithic SiC. Detail of the microscopy of the REABond joints for BFG SiC/SiC had been reported previously[8]. Therefor more emphasis will be placed on showing micrographs of joined GE SiC/SiC. To obtain special joints for microscopy, two substrate bars were stacked one on the other as shown in the upper right corner of Figure 1. The polished cross-section of the joint of the fully bonded GE SiC/SiC is shown in Figure 4. A good quality joint is seen across the full 24 mm length of the bonded substrates. The joint is uniform with no gaps or porosity. Close up views of the different joints are shown in Figure 5 where the left image is of GE SiC/SiC joined with the standard REABond tape, the middle image is GE SiC/SiC joined with the REABond tape with 5 wt.% SiC nanotubes, and the right is BFG SiC/SiC joined with the standard REABond tape. The joint of the BFG SiC/SiC substrates shows that even though there are wide and narrow gaps along the paired CMC surfaces, the REABond interlayer is able to fill in this uneven surface to give a consistent joint. The gap goes from about 150 micron at its most narrow span to about 300 microns at the widest span. In comparing the GE SiC/SiC joints with and without the added nanotubes, it is seen in the joint formed with the REABond tape w/ 5 wt.% SiC nanotube there is a dispersed phase. Greater detail of the joint formed with nanotubes is shown in Figure 6. The dispersed phase can be seen throughout the joint. In the close up view, three phases are labeled which were identified through EDS as a Si-rich phase, a SiC phase, and a Si-Hf-C phase. The SiC regions have a grain shape rather than original nanotube shape. X-ray diffraction of the supplied SiC nanotubes revealed that the nanotubes were not purely SiC but rather consisted of a SiC phase and a carbon phase (Figure 7). It is believed that during processing of the joints, the Si-rich phase in the REABond reacted with the carbon in the nanotubes. Therefor the nanotube structure was lost and the goal of having a reinforced joint with composite like properties was not achieved.

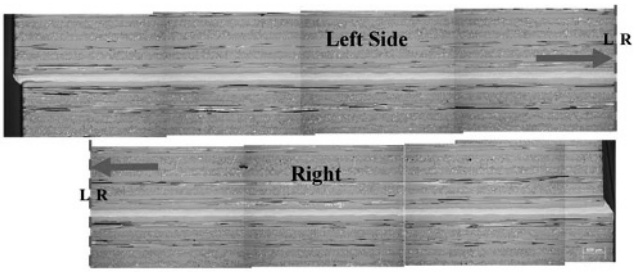

Figure 4. Optical micrograph of the entire 24 mm long cross-section of two fully paired GE HyperComp SiC/SiC substrates. Joining was done with two REABond tapes.

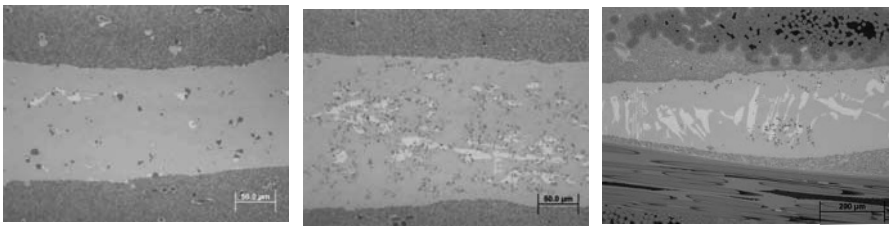

Figure 5. Cross-sections of as processed joints: GE SiC/SiC joined with the 2 layers of standard REABond tape (left), GE SiC/SiC joined with 2 layers of the REABond tape with 5 wt.% SiC nanotubes (middle), BFG SiC/SiC joined with 3 layers of the standard REABond tape (right).

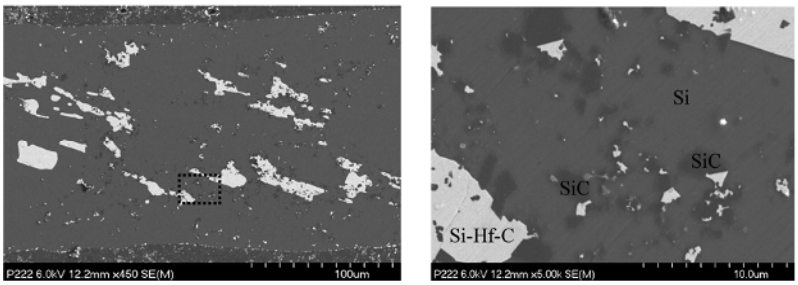

Figure 6. FE SEM micrographs of the same region at different magnifications for the GE SiC/SiC joined with 2 layers of the REABond tape with 5 wt.% SiC nanotubes.

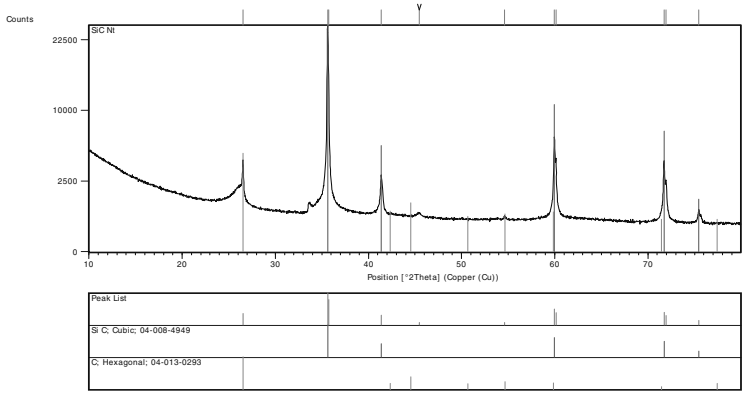

Figure 7. Results from x-ray diffraction analysis of the supplied "SiC" nanotubes showing that there was also a carbon phase present in the material.

The joined crossbars were tested in tension and shear according to the ISO-13124 test standard. The ultimate strengths are shown in Figure 8 for tensile (right) and shear (left) tests of the four material and interlayer combinations: GE SiC/SiC joined with REABond, GE SiC/SiC joined with REABond with 5 wt.% SiC nanotubes, BFG SiC/SiC joined with REABond, and monolithic SiC joined with REABond. The CMC materials had lower than expected tensile and shear strengths. In order to avoid composite property issues such as low interlminar properties, crossbars were also tested of monolithic SiC joined with REABond. Tensile strengths for all materials ranged from 3 MPa to less than 7 MPa. The REABond joined GE SiC/SiC had the lowest strength while the monolithic SiC joined with REABond had the highest. The nanotube reinforced joints seemed to provide some benefit in tension. The shear strengths were higher and ranged from 10-37 MPa overall with the monolithic SiC joined with REABond having the lowest strength and the GE SiC/SiC joined with REABond having the highest strength. The strengths seemed low considering that in previous result using an alternate test method, single lap offset, apparent shear strengths of 100 MPa were observed for joined SiC fiber reinforced substrates[8].

The different sample sets failed under different mechanisms. However, it appears that failures did not occur entirely in the join region and maybe not even partially. This suggest that the joints could have potentially higher strengths than those recorded. However, the premature failure in the substrates did not allow the joint material to be fully pushed to its limits.

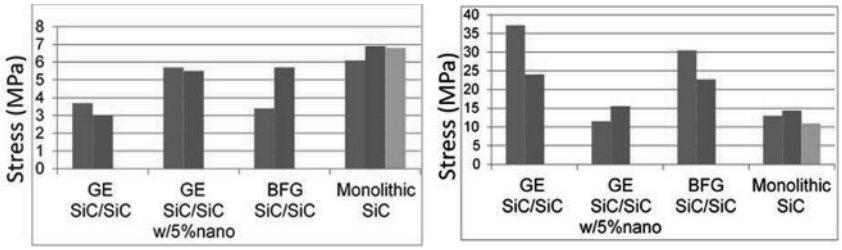

Figure 8. Ultimate strength results from ISO-13124 tests for the tensile stress state (left) and the shear stress state (right). Two crossbar samples were tested for the CMC materials while three were tested for the monolithic SiC for each stress state.

Figure 9 shows how some of the materials failed in tension. The image on the left is of the BFG SiC/SiC joined with REABond. A corner view of the 8 mm x 8 mm crossover bond area is seen with failure within the CMC down to one of the fiber ply layers. The GE materials also failed in a similar manner, either in a ply layer or in the top coat laminate layer. The joined monolithic substrates avoided the low interlaminar property issues observed in the CMCs, however failure occurred in one of the extended arms of the crossbar as shown in the micrograph on the right. Examples of the failures that occurred during the shear tests are shown in Figure 10. Failures occurred in a similar fashion as for tension, the GE SiC/SiC bonded substrates failed in a fiber laminate layer and the monolithic bonded substrates again failed in an extended arm of the crossbar. However, the BFG SiC/SiC crossbar joined with REABond did not fail in a manner in which the substrates separated. Instead failure occurred at the back surface of one of the CMC substrates and shown in Figure 10 (top-right). The premature failures, low strengths, and fractures in the substrates demonstrate the challenges in having well developed and reliable test methods for fully characterizing the mechanical properties of joints for ceramic and CMC materials.

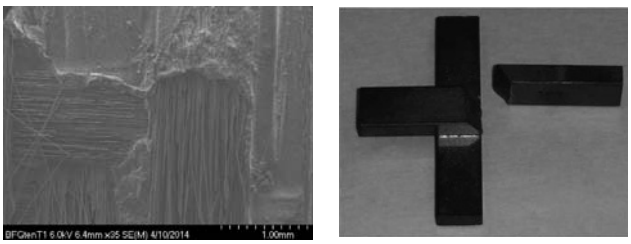

Figure 9. FE SEM micrograph of the fracture surface of BFG SiC/SiC joined with REABond (left) and a macroview of the monolithic SiC joined with REABond (right) after tension tests.

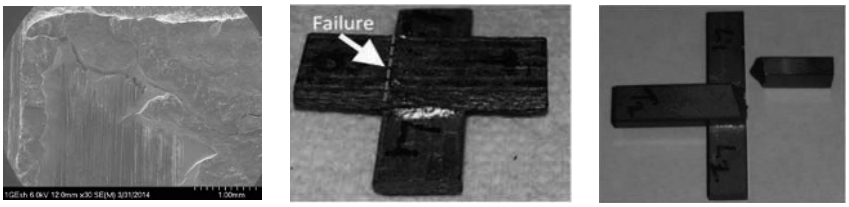

Figure 10. FE SEM micrograph of the fracture surface of GE SiC/SiC joined with REABond (left) and a macroviews of the BFG SiC/SiC joined with REABond (middle), the monolithic SiC joined with REABond (right) after shear tests.

These wide variations in the distribution of stresses within the bond region were characteristic for both cross-bonded specimen configurations. This wide variation in the stress distribution is likely contributed to the thinner section of the cross bar specimen which allow for greater out of plane displacement due to bending when subject to a transverse load. The bar section's aspect ratio for the cross-sectional area is other than 1 which is suggested for the test standard. When the cross-bonded specimen are oriented for the shear strength bond test a similar complication occurs. However, it is in the form of undesirable out-of-plane displacement which results in other than pure shear during testing. The vertical load on the vertical bar is off-centered to the neutral axis of the test specimen and as a result of the setup produces bending which induces a normal stress as well as a shear stress within the bond region (Figure 12). The above behavior for shear strength tests makes it difficult for calculating the strength of the bond by way of conventional means. Since these types of displacements cannot be fully eliminated determining how much out-of-plane displacement is excessive is yet to be established since percent bending during testing was not monitored.

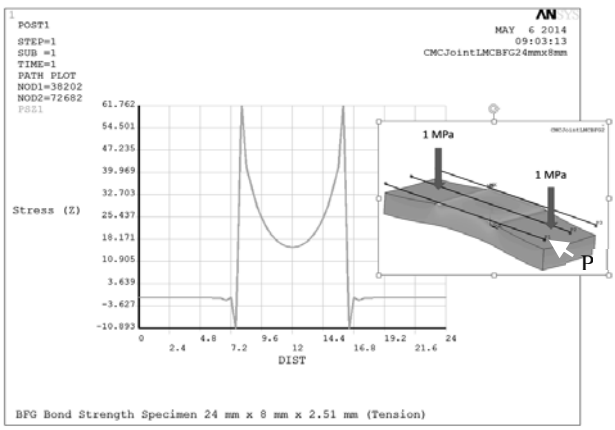

Figure 11. Typical tension stress results within the bond region for cross bar ceramic joint specimen. Plot of stress distribution along path P1.

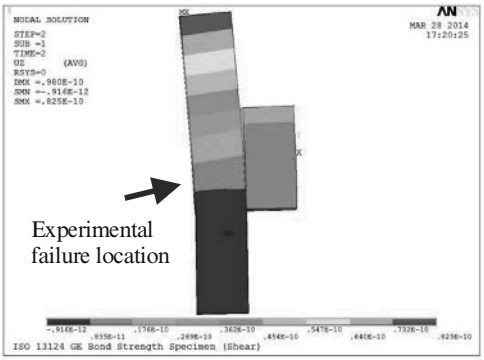

Figure 12. Shear test bond strength displacement plots for cross-bonded specimen.

CONCLUSIONS

The REABond joining approach which used green tapes containing Si-8.5Hf eutectic phase alloy powders was shown to be an effective joining approach for obtaining good quality bonds. REABond tapes were successfully integrated with 5 wt.% SiC nanotubes. The nanotubes were well dispersed throughout the tapes. However, during processing of the joints, a minor carbon phase in the nanotubes reacted with a Si-rich phase in the joint region. The SiC nonotubes lost their shape and became grain shaped. The tensile and shear strengths for all four substrate and REABond interlayer combinations seemed to be lower than would be expected. Low interlaminar properties of the CMCs seemed to contribute to the low strengths with failures observed in the composite layers rather than in the joint region. Also, the joined monolithic SiC crossbars failed at one of the extended arms of the crossbar rather than failing in the joint. The results suggest that the joints potentially had higher strengths than measured but samples failed prematurely in the substrates.

The purpose of the finite element analysis was not to predict when failure of the bond joint occurs but to establish the stress distribution within the bond to aid in determining how to calculate the stress at failure. Typically that stress is determined by dividing the recorded load at failure by the cross-sectional area of the bond region. The finite element results show that the stress at the edge of the bond region could be as high as 30 times the nominal stress which is 2 MPa.

Cross-bonded specimen tensile ceramic bond test shows a wide variation in the stress distribution within the bond region when a downward load is applied to the bar. It may be more beneficial to reverse the loading such that a compressive load is initially created within the bond. Once bending of the bars develop, tensile stresses are created within the center region of the bond thereby significantly reducing the edge effects. When shear test is conducted the out-of-plane displacement occurs that induce other than pure shear stresses. The test specimen or test fixture should be modified in order to avoid bending due to off centering of applied load on test specimen. The experimental results and the finite element results show the challenges in applying ISO-13124 to the testing of joined ceramics and CMCs. Further analysis of the standard is needed as well as possible modifications to the tests or new interpretations of experimental results such as a multiplication factor to account for the high stresses at the edges of the joint region.

ACKNOWLEDGEMENT

The authors would like to thank Ronald Phillips of Vantage Partners, LLC in Cleveland, OH for conducting the tensile and shear tests and Gregory L. Piper of Jacobs Technology in Cleveland, OH for designing the fixtures for the tensile and shear tests. This work was supported by the Transformational Tools and Technologies ((TTT) Project under the NASA Transformative Aeronautics Concepts Program.

REFERENCES

1. Josh Kimmel, Narendernath Miriyala, Jeffrey Pricea, Karren More, Peter Tortorelli, Harry Eaton, Gary Linsey, Ellen Sun "Evaluation of CFCC Liners with EBC After Field Testing in a Gas Turbine," Journal of the European Ceramic Society, 22, 2769–2775 (2002).

2. R. Naslain, "Design, Preparation and Properties of Non-Oxide CMCs for Application in Engines and Nuclear Reactors: An Overview," Composites Science and Technology, 64, 155–170 (2004).

3. Mark van Roode, Jeff Price, Josh Kimmel, Naren Miriyala, Don Leroux, Anthony Fahme and Kenneth Smith, "Ceramic Matrix Composite Combustion Liners: A Summary of Field Evaluations," J. Eng. Gas Turb. Power, 129, 21–30 (2007).

4. Michael C. Halbig, Martha H. Jaskowiak, James D. Kiser, and Dongming Zhu, "Evaluation of Ceramic Matrix Composite Technology for Aircraft Turbine Engine Applications," 51st AIAA Aerospace Sciences Meeting including the New Horizons Forum and Aerospace Exposition, 07 - 10 January 2013, Grapevine, Texas, Vol. 9, pp. 7964-7974.

5. BS-ISO-13124:2011, "Fine ceramics (advanced ceramics, advanced technical ceramics). Test method for interfacial bond strength of ceramic materials," May 12, 2011.

6. Michael C. Halbig and Mrityunjay Singh, "Diffusion Bonding of Silicon Carbide for the Fabrication of Complex Shaped Ceramic Components," Ceramic Integration and Joining Technologies: From Macro- to Nanoscale, Eds. M. Singh, T. Ohji, R. Asthana and S. Mathur, John Wiley & Sons, 2011.

7. Michael C. Halbig, Mrityunjay Singh, and Hiroshi Tsuda, "Integration Technologies for Silicon Carbide-Based Ceramics for Micro-Electro-Mechanical Systems-Lean Direct Injector Fuel Injector Applications," International Journal of Applied Ceramic Technology, July/August 2012, Volume 9, Issue 4, Pages 677–687.

8. Michael C. Halbig, Mrityunjay Singh, and Craig E. Smith. "Joining of SiC/SiC Ceramic Matrix Composites Using Reabond Technology," Design, Development, and Applications of Structural Ceramics, Composites, and Nanomaterials: Ceramic Transactions, Volume 244: 39-51.

9. G.S. Corman, and Luthra, K.L., "Silicon Melt Infiltrated Ceramic Composites (HiPerComp™)," in Handbook of Ceramics and Glasses, ed. N. Bansal, Kluwer Academic Publishers, Boston, 2005, pp. 99-115.

10. Janet Hurst, "Chapter 9 - Boron Nitride Nanotubes, Silicon Carbide Nanotubes, and Carbon Nanotubes-A Comparison of Properties and Applications," Pages 267-287, Nanotube Superfiber Materials-Changing Engineering Design, Edited by: Mark J. Schulz, Vesselin N. Shanov, and Zhangzhang Yin, 2014.